

Ionic Aggregates in Steam. 2. Standard Chemical Potentials

Roberto Fernández-Prini[†]

Unidad Actividad Química, Comisión Nacional de Energía Atómica, Av. Libertador 8250, 1429-Capital Federal, Argentina, and INQUIMAE, Facultad de Ciencias Exactas y Naturales, Universidad de Buenos Aires, 1428-Capital Federal, Argentina

Received: June 19, 1997; In Final Form: October 13, 1997[®]

KCl and NaCl in model steam have been studied by molecular dynamics. The distribution of H₂O around the ions has been established and their orientation compared to that predicted for point dipoles. Residual chemical potentials for the ionic species in steam have been calculated from the results of the simulations using the Kirkwood coupling parameter method. With this information it has been possible to calculate the association constant of ions into pairs and the solubility of the solid salts in steam. The results are in a good agreement with the scarce experimental information available. Thermodynamic quantities for ions in steam are compared with those for the hydration of the same ions in water at different temperatures.

1. Introduction

The behavior of ions in polar liquids has been thoroughly studied both by theoretical and experimental means. Not only are thermodynamic and transport properties for these systems well-known now but also the structural details have been worked out by experiment and computer simulation.^{1–3} In spite of this intense activity there are two thermodynamic regions of the fluid-phase diagram of polar solvents that are not very well characterized yet; both regions have a high fluid susceptibility, i.e. a large compressibility. Fluids exhibit a large susceptibility in the near-critical region and in the low density vapor phase, and as recognized by Wood and co-workers,^{4,5} the Debye–Hückel model is not directly applicable to these cases. However the reasons for the high compressibility of fluids in the two regions are different. Near-critical fluids, which have a low liquidlike density of, about, one-third of their triple-point density, are very susceptible due to the long-range fluctuations of local density, which have an increasing range as the system approaches its critical point.⁶ On the other hand, vapors are very susceptible because the fluid has a very low packing fraction.

The structure and thermodynamic properties of multicomponent fluids, including solvation phenomena, are dominated by different interaction regimes depending upon the fluid density.⁶ Repulsive interactions dominate the behavior in triple-point fluids, while attraction prevails in fluids having lower density (starting somewhere below half the triple-point density). This difference is also observed in the solvation dynamics which, for highly interacting solvent molecules like H₂O, is dominated by solvent rotations and librations when the fluid's packing fraction is high (triple-point density), but as its density decreases, the translational component contributes increasingly to the solvation dynamics.⁷ The translation of molecules is the mechanism that leads to a local increase in solvent density surrounding the ions, a characteristic of ion solvation in low-density fluids.⁸

There is also practical interest in knowing the behavior of ionic solutes in steam because salts carried by steam offer a route for the transport of ionic compounds in hydrothermal

processes which afterward may undergo several chemical reactions, including corrosion, in industrial and natural hydrothermal processes.

Recently new measurements of NaCl conductivity in supercritical water⁹ showed that at low density and temperature this salt is more dissociated than previously established.¹⁰ Analysis of the scarce thermodynamic data available for the solubility of salts in steam also suggested that salts were more dissociated in steam than previously thought.¹¹ For these reasons we decided to study the behavior of ionic species in steam. However, since the experimental conditions necessary to obtain meaningful information in this medium are very demanding due to the low concentration of the salts, we have resorted to molecular simulation in order to carry out this study.

In the first part of this research, to be denoted as part 1,⁸ we have reported the equilibrium configurations of ionic aggregates in model steam that resulted from the molecular dynamics study. It was shown that the presence of charged and uncharged ionic aggregates of KCl in steam leads to a strong inhomogeneity in the distribution of water molecules surrounding the ionic species. Close to the ions there is a considerable increase in the local density of H₂O molecules which attains values close to those typical of a liquid phase. In the present work the study has been extended to cover more thermodynamic points for KCl, and due to the lack of reliable experimental information for this salt in steam, two thermodynamic points for NaCl in steam have also been analyzed. Two aspects are presented here and discussed: the orientational distribution of water molecules surrounding the free ions is considered and compared to that predicted for spherical H₂O having a point dipole at its center; secondly, values of the standard chemical potentials of free ions and ion pairs have been calculated for KCl and NaCl in steam. This information has been used to determine values for the equilibrium constant describing the association of free ions into ion pairs in steam and also for the solubility and enhancement factor for the salts in steam.

2. Interaction Potential and Simulation Procedure

The effective Hamiltonians employed in this work to describe intermolecular interactions were the simple point charge (SPC) model for water,¹² and a potential of the Huggins-Mayer type,¹³

[†] Member of Carrera del Investigador, CONICET. E-mail: rfrprini@cnea.edu.ar.

[®] Abstract published in *Advance ACS Abstracts*, December 1, 1997.

TABLE 1: Thermodynamic States of SPC Steam

state	salt	<i>T</i> (K)	ρ^0 (nm ⁻³)	<i>p</i> (MPa)	ϵ
I	KCl	500	0.436	2.6	1.10
II	KCl	500	0.217	1.38	1.05
III	KCl	573	0.738	5.0	1.16
IV	KCl	623	0.578	4.53	1.11
V	NaCl	623	0.578	4.53	1.11
VI	NaCl	623	1.595	10.0	1.31
VII	KCl	450	0.151	0.90	1.01

having an exponential repulsive term and a Coulombic term, was used to describe the ion–ion interactions. The water–ion potential was modeled as a sum of a (6–12) Lennard-Jones term plus a simple Coulombic tail.¹⁴ Details of the intermolecular potentials and values of the parameters used have been given elsewhere.¹⁵

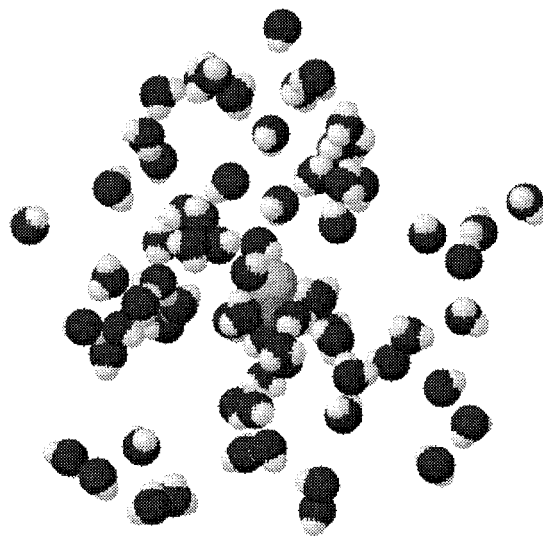
The fluid system where the ions are immersed has very low density; hence in order to perform an efficient molecular dynamics simulation study of this system, it was necessary to adopt a special procedure. Use of the conventional procedure that employs periodic boundary conditions would have required a very large simulation cell, and even then it would have been difficult to avoid the effect of the neighboring replicas which also contain ions, due to the long-range nature of the Coulombic interactions and the low dielectric screening power of the fluid. The simulation procedure used here has been described in detail elsewhere.⁸ Briefly, it consists of restricting the simulation to a sphere 2.0 nm radius surrounding the ionic aggregates; H₂O molecules collide against its surface and penetrate the sphere. In the original procedure H₂O molecules entered the simulation sphere at the average collision rate corresponding to the temperature and density of the run; in the present work the penetration strategy was modified so that the time when a new H₂O molecule penetrated the simulation sphere was chosen with the Poisson distribution corresponding to the average collision time.¹⁶ The simulation step was of 1 fs, and the SHAKE algorithm¹⁷ was used to handle constraints resulting from the intramolecular bonds in the solvent molecules and those acting on the interionic distances for the case of ion pairs. The quantities calculated for each run were averages taken for a total simulation time of 1 ns, except at the highest temperature and pressure, where it was 0.8 ns.

One condition which must be fulfilled to validate this simulation procedure is that the local number density of H₂O must approach smoothly inside of the simulation sphere the value of the density of bulk steam. This was taken to imply that all the interactions of ions with H₂O beyond that predicted by the continuum model are accounted for. At the highest temperature and density of steam that was studied in the present work, the local density of H₂O became equal to that of bulk steam (within $\pm 1\%$) at a distance of 1.3 nm from the ions.

The thermodynamic states of model SPC steam that have been studied were characterized by the values of *T* and ρ reported in Table 1; the pressure *p* given in the fifth column corresponds to that of real steam for those *T*, ρ values. Table 1 also reports values of the dielectric constant, ϵ , of real H₂O for the same states;¹⁸ these values were used to correct the standard chemical potential of the free ions as explained below. Simulation runs were performed for the two free ions and for the ion pairs. For NaCl at the highest density of steam, triplet ions were also studied.

3. H₂O in the Equilibrium Configurations

It was noted in part 1 that the ionic aggregates were surrounded by a large number of H₂O molecules; the local

**Figure 1.** Equilibrium configuration for Na⁺–Cl[–] in state VI.**TABLE 2: Number of H₂O Molecules in the Simulation Sphere and Mean Ionic Separation of the Ions in the Pairs**

state	n_s^0	Δ_+	Δ_-	Δ_{\pm}	$r_{\pm}(\text{aq})/\text{nm}^a$
I	14.8	12.7	12.9	9.9	0.300
II	7.3	8.2	9.5	7.3	0.296
III	24.7	9.7	7.3	6.7	0.294
IV	19.4	7.8	6.7	4.6	0.289
V	19.4	8.6	6.7	4.9	0.257
VI	53.5	17.7	17.5	16.0	0.267

$$^a r_{\pm}(\text{KCl}, \text{g}) = 0.267 \text{ nm}; r_{\pm}(\text{NaCl}, \text{g}) = 0.231 \text{ nm}.$$

density close to the ions had a value that was 70% of the density of bulk water at room temperature, i.e. typical of a liquid phase. Consequently, the radial distribution function of H₂O surrounding the ions exhibited a very large first peak. This feature is also present in the new thermodynamic states which have been studied now. Figure 1 shows, as an example, a representative microconfiguration of the (Na⁺–Cl[–]) ion pair surrounded by SPC-H₂O's in state VI; the increase in local solvent density close to the ion pair is evident. Water molecules close to the ionic species show strong intermolecular interactions (hydrogen bonding); in the configuration illustrated in Figure 1 these interactions lead to the formation of strands of H₂O which cluster around the ion pair. This example emphasizes the role of the charge distribution on the atoms of SPC-H₂O.

The number of H₂O's inside the simulation sphere containing the ionic species *i* is denoted by n_{si} , and by n_s^0 when no ions are inside the sphere. Table 2 reports for each system studied the values of n_s^0 and of $\Delta_i = n_{si} - n_s^0$, the excess of H₂O molecules in the sphere containing species *i*. The average distances between anion and cation in the ion pairs, $r_{\pm}(\text{aq})$, are also given in Table 2. The values of Δ_i are quite large, being larger for free ions than for pairs, but in no case was Δ_i found to be negligible. When two ions form a pair, more than half of the water molecules interacting with the free ions are expelled from the simulation sphere. This change in n_{si} produces a relative stabilization of the free ions by steam and is an important contribution to the Gibbs energy of association. The relative increase in n_{si} for a given ionic species is observed to be larger at low temperature and density and somewhat larger for Na⁺ than for K⁺ ions. The average $r_{\pm}(\text{aq})$ also decreases with increasing temperature and steam density, but for all the states studied it is appreciably larger than $r_{\pm}(\text{g})$ calculated with the Mayer–Huggins potential for the pure salt vapor (cf. Table 2).

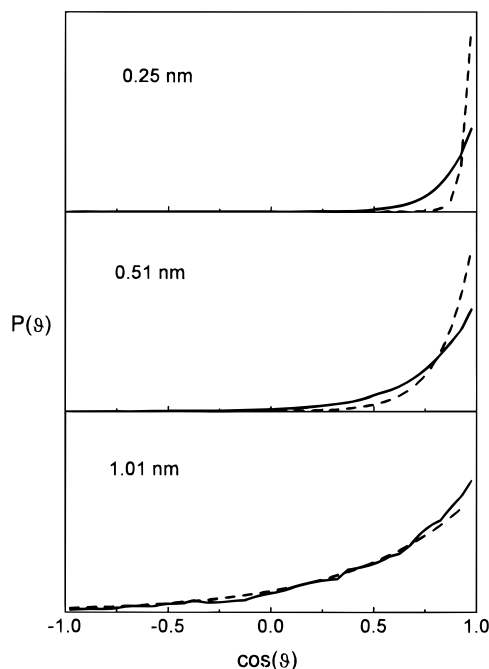


Figure 2. Relative values of the normalized distribution of the orientation of H₂O surrounding K⁺ in state VII for the distance from the ion indicated on each panel. Full line: from simulation. Dashed line: Langevin distribution.

We have determined for K⁺ and Cl[−] ions the average orientation of the SPC-water molecules surrounding the free ions and calculated the normalized distribution function for dipole orientation, $P(r, \cos \theta)$. It has been compared with that obtained with the Langevin distribution function, which is given by¹⁹

$$P(r, \cos \theta) d\theta = \exp(\beta \mu_{\text{H}_2\text{O}} E_i(r) \cos \theta) \sin \theta d\theta \quad (1)$$

where θ is the angle between the dipole of an H₂O molecule and the distance vector going from the center of the ion to that H₂O molecule and β is the reciprocal of Boltzmann's constant times the temperature. $E_i(\mathbf{r})$ is the electric field vector at distance \mathbf{r} from ion i , and $\mu_{\text{H}_2\text{O}}$ is the dipole moment of SPC-H₂O. The electric field is given by $E_i(\mathbf{r}) = q_i \mathbf{r}/r^3$, where q_i is the charge of the ion.

$P(r, \cos \theta)$ as function of $\cos \theta$ is illustrated in Figure 2 for K⁺ and in Figure 3 for Cl[−] in state VII. In each figure we have plotted $P(r, \cos \theta)$ at three distances from the ions; the ordinate scale is arbitrary to simplify the illustration since the main interest is to compare the simulation results with those of the point dipole model. It is quite clear that for the first two panels in each figure there are large differences between the Langevin distribution of point dipoles and $P(r, \cos \theta)$ resulting from the molecular dynamics runs. For state VII this difference was found to be negligible for $r > 0.7$ nm from the central ion; at the same distance the radial distribution function of water molecules surrounding the free ions became unity for the same state.⁸ Another difference with the point dipole in a sphere model of H₂O is worth noting: for Cl[−] the most probable orientation of the water molecules close to its surface corresponds to one hydrogen atom pointing toward the center of the Cl[−] ion; that is, the most probable value of θ is 127.7°. Kebarle and co-workers²⁰ observed the same nonsymmetrical orientation for the H₂O molecules surrounding halide ions in small $[\text{X}^-(\text{H}_2\text{O})_n]$ clusters.

In part 1 it was noted that the radial distribution function of SPC-H₂O surrounding an ion was very different from that

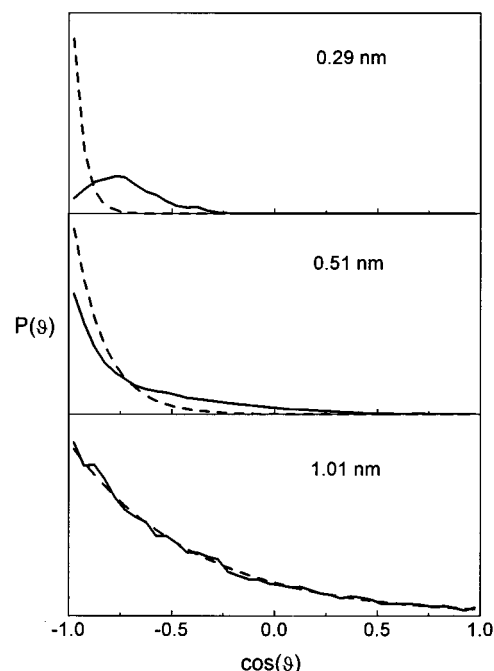


Figure 3. Relative values of the normalized distribution of the orientation of H₂O surrounding Cl[−] in state VII for the distance from the ion indicated on each panel. Full line: from simulation. Dashed line: Langevin distribution.

obtained for this model H₂O when Coulombic interactions among the water molecules were suppressed; that is, water–water interactions were restricted only to the Lennard-Jones term in the SPC Hamiltonian. In this case the water molecules crowded even closer to the ion, and $P(r, \cos \theta)$ for the point dipole spherical water molecules next to the K⁺ ion was found to differ much less from that predicted by a Langevin distribution. This evidence indicates that the different behavior observed in steam for SPC-H₂O and the point dipole H₂O is not due to an excluded volume effect in the neighborhood of ions but rather to the Coulombic interactions between the neighboring water molecules that determines the orientational arrangement of the H₂O molecules. This is also clear in the snapshot configuration shown in Figure 1.

4. Calculation of the Standard Chemical Potential of the Ionic Species in Steam

The Kirkwood coupling parameter method²¹ was found very convenient to calculate from the results of the simulation runs the contribution to the chemical potentials due to the intermolecular interactions, i.e. the residual chemical potentials.²² The method consists in calculating the average water–ion interaction energy $\langle \Phi_{is} \rangle_\lambda$ for different values of a coupling parameter λ . To vary the coupling between H₂O and the ions, we have made the charge on the ions equal to λq_i ; when $\lambda = 1$, ions are fully charged and interact with water molecules; when $\lambda = 0$, there are no interactions between the H₂O molecules and the ionic species. The residual chemical potential at infinite dilution of species i , $\mu_i^{\infty, \text{res}}$, is then obtained by integrating the average interaction energy between $\lambda = 0$ and $\lambda = 1$; that is

$$\mu_i^{\infty, \text{res}} = \int_0^1 \langle \Phi_{is} \rangle_\lambda d\lambda \quad (2)$$

Simulation runs were performed reducing progressively the charge on the ionic species until $\lambda = 0.4$, and $\langle \Phi_{is} \rangle_\lambda$ was calculated for each value of the coupling parameter. The

average ion–water energy of interactions for $\lambda \leq 0.4$ was about 5% of $\langle \Phi_{is} \rangle_{\lambda=1}$. The values of $\langle \Phi_{is} \rangle_{\lambda}$ were then extrapolated smoothly until this quantity became zero; this usually happened for values of λ close to 0.3. For the ion pairs it was not possible to make simulations with $\lambda < 0.4$ because the two ions drifted away from each other during the runs due to the low attraction existing between them. This problem was even more severe for the aggregates having three ions; one ion was expelled from the simulation sphere and a neutral pair remained whenever $\lambda \leq 0.7$. It should be noted that even for the fully charged ions in a triplet, the simulation runs for state VI showed that many microconfigurations really corresponded to a pair of ions that were very close to each other and separated from the third ion by a longer distance. Hence no calculations of chemical potentials for the triplets were attempted.

In this study the fluid has a packing fraction that is considerably smaller than that of triple point water; hence the repulsive contribution to $\mu_i^{\infty, \text{res}}$ (cavity formation) arising in dense fluids when the charge coupling parameter is zero will be negligible.²³ Consequently $\langle \Phi_{is} \rangle_{\lambda=0} \approx 0$. This observation lends support to the use of an extrapolation procedure. The extrapolation procedure was checked for free ions in order to verify that the results coincided with those of the simulation runs when λ was reduced down to a charge 0.1. Therefore the values of the residual chemical potential obtained are considered to be correct within 2%.

The application of Kirkwood's method requires that only the configurational integral be affected by changes in λ . For the ion pairs as λ decreased, the average distance between the ions was observed to increase; consequently it was necessary to constrain the distance between the pair of ions to its average value when the two ions were fully charged in steam, $r_{\pm}(\text{aq})$.

For the ionic species in steam, the chemical potential at infinite dilution is given by

$$\mu_i^{\infty}(\text{aq}, T) = \mu_i^{\ominus}(T) + \mu_i^{\infty, \text{res}} \quad (3)$$

where $\mu_i^{\ominus}(T)$ is the standard chemical potential of species i in the gas phase when no water is present. The calculation of $\mu_i^{\infty, \text{res}}$ with eq 2 gives the contribution of the interactions between the ionic species and all the H_2O molecules contained inside the simulation sphere. Another small term should be added as a correction; it arises from the work necessary to charge the simulation sphere in bulk steam. This electrostatic work depends on the bulk dielectric constant of steam and can be calculated from the expressions derived with the continuum model.²⁴ For the free ions, the correction is given by the Born equation,

$$\mu_i^{\text{res, corr}} = -\frac{\epsilon - 1}{\epsilon} \frac{q_i^2}{2R} \quad (4)$$

where $R = 2.0$ nm is the radius of the simulation sphere. For the ion pair the correction is given by the electrostatic interaction with the dipole μ_{IP} formed by the two ions separated at their average distance $r_{\pm}(\text{aq})$, placed at the center of the simulation sphere. Hence,

$$\mu_{\pm}^{\text{res, corr}} = -\frac{(\epsilon - 1)\mu_{\text{IP}}^2}{(2\epsilon + 1)R^3} \quad (5)$$

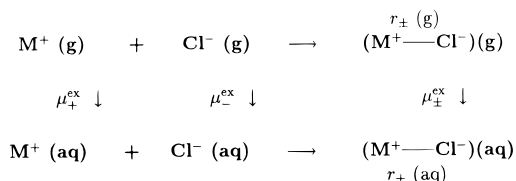
This correction to $\mu_{\pm}^{\infty, \text{res}}$ turned out to be negligible, as observed by Cui and Harris²³ in their simulation study of NaCl pairs in supercritical water. One more correction is necessary

TABLE 3: Residual Chemical Potentials (kJ mol^{-1}), Residual Internal Energy (kJ mol^{-1}), and Association Constant of Ionic Species in Steam

state	μ_+^{res}	μ_-^{res}	μ_{\pm}^{res}	U_+^{res}	U_-^{res}	U_{\pm}^{res}	$\log K_c$
I	-112.3	-83.4	-86.5	-422.8	-362.3	-320.5	30.99
II	-99.7	-67.1	-63.4	-363.7	-314.3	-290.8	33.74
III	-99.0	-74.8	-63.1	-391.1	-321.5	-271.6	25.55
IV	-88.5	-62.2	-47.1	-356.4	-277.6	-227.3	26.05
V	-136.4	-62.2	-66.4	-503.7	-277.6	-272.2	28.31
VI	-168.5	-101.9	-98.0	-582.3	-385.9	-342.4	23.34

in order to calculate the difference between the standard chemical potentials in vacuo and in steam for the ion pairs. The average distance separating cation and anion is different in steam and in vacuo, as observed by the values reported in Table 2. To make this correction, it is necessary to calculate the work of separation of the two ions in the pair from $r_{\pm}(\text{g})$ to $r_{\pm}(\text{aq})$ in vacuo. This value has been equated to the energy of separation of both ions calculated with the potential of intermolecular interaction between the two ions, thus assuming that the entropic contribution to this process would be very small. The values obtained for $\mu_i^{\infty, \text{res}}(\text{aq}, T)$ are reported in Table 3. This table also gives the residual internal energy at infinite dilution $U_i^{\infty, \text{res}}$ equal to $\langle \Phi_{is} \rangle_{\lambda=1}$, plus the corrections detailed above.

The standard chemical potentials have been used to calculate the thermodynamic quantities corresponding to two processes: the association of free ions into pairs and the solubility of the solid salt in steam. The following reaction scheme summarizes the thermodynamic cycle employed to calculate the ion association process.



The Gibbs energy of association is given by

$$\Delta_{\text{Assoc}} G(\text{aq}) = \Delta_{\text{Assoc}} G(\text{g}) + \mu_{\pm}^{\infty, \text{res}} - \mu_+^{\infty, \text{res}} - \mu_-^{\infty, \text{res}} \quad (6)$$

The term $\Delta_{\text{Assoc}} G(\text{g})$ is the Gibbs energy of association of the gaseous ions in vacuo; values for this quantity were obtained from the JANAF compilation.²⁵ They refer to the standard state of gaseous species at the standard pressure p^{\ominus} , e.g. $\mu_i^{\ominus}(\text{g}, p^{\ominus})$; it is necessary to convert them to the molarity scale since that is the one that corresponds to the statistical mechanics derivation of the Kirkwood method.²¹ The change of scale was made using the expression

$$\mu_i^{\ominus}(\text{g}, p^{\ominus}) = \mu_i^{\ominus}(\text{g}, c^{\ominus}) - RT \ln RT \quad (7)$$

where c^{\ominus} represents the standard molarity. Thus the values of $\Delta_{\text{Assoc}} G(\text{aq})$ and also those of the logarithm of the association constant K_c which is related to the previous quantity by

$$\Delta_{\text{Assoc}} G(\text{aq}) = -RT \ln K_c \quad (8)$$

were calculated. They are given in Table 3.

The standard chemical potentials obtained from the results of the simulation runs have been used also to calculate the solubility of the solid salt in steam. The condition of equilibrium between the solute in the pure solid and in steam relates the chemical potentials of MCl in both phases; that is,

TABLE 4: Solubility of Solid KCl and NaCl in Steam

state	$10^8 x$		$10^{-4} \epsilon$
	<i>a</i>	<i>b</i>	
I	0.058	420(1)	19.6
II	0.061	94(1)	11.0
III	3.74	$2.8 \times 10^3(1)$	3.08
IV	6.91	250(1)	0.132
V	28.1	470(1); 5.2(2)	2.04
VI	895	$3.8 \times 10^3(1)$; 340(2)	143.4

^a This work. ^b (1) ref 29. (2) ref 27.

$$\mu_{\text{MCl}}^*(s) = \mu_{\text{MCl}}(\text{aq}) \quad (9)$$

The MCl salts studied in this work are fairly associated in steam, as shown by the values reported in Table 3, and very strongly in the absence of steam; hence the vapor pressure of MCl in steam may be calculated, as for the pure salt, only on the basis of the ion pair chemical potential. Since we have, for MCl in phase α ,

$$\mu_{\text{MCl}}(\alpha) = \mu_{\text{MCl}}^\ominus(\alpha, p^\ominus) + RT \ln \frac{p_{\text{MCl}}}{p^\ominus} \quad (10)$$

the following expression for the enhancement factor ϵ , the ratio between the solubility of MCl in the presence of steam to that in the absence of H_2O , which is given by its vapor pressure, p_{MCl}^* , may be derived:

$$RT \ln \epsilon \equiv RT \ln \left(\frac{p_{\text{MCl}}(\text{aq})}{p_{\text{MCl}}^*} \right) = -\mu_{\pm}^{\text{res}}(\text{aq}) \quad (11)$$

The values of the equilibrium mole fraction of MCl in steam and the enhancement factors are reported in Table 4.

5. Discussion

The experimental information about the behavior of ions in steam (subcritical temperatures) is very scarce. With regard to the association of ions, data from conductivity measurements exist for KCl²⁶ and for NaCl^{9,10} in supercritical water. These studies cover a wide range of temperatures and water densities, but they do not extend below the critical density of water, which is still much higher than the densities of the states studied here for steam. They have shown that the behavior of K_c for the salts as a function of density is almost linear for water densities larger than 0.3 g cm^{-3} .

A thorough analysis of the data available for the binary NaCl– H_2O system over wide ranges of p , V , T has been published by Pitzer and Pabalan;²⁷ they considered that NaCl is completely associated in steam. On the other hand, an analysis of the limited information available for the distribution of NaCl and KCl between steam and water⁶ led us to believe that these salts were more dissociated in steam than previously thought. This impression found some support in the higher dissociation found for NaCl in high-temperature water found by Ho et al.⁹ and in simulation results that indicated an important stabilization of free ions by H_2O molecules due to the effective screening of the interionic interaction of the pair of ions found in small water clusters.²⁸ However the values of the association constant found in the present study indicate that even when MCl is less associated than might have been expected, for all practical purposes in the thermodynamic states covered in this work, they are essentially associated, in agreement with the assumption of Pitzer and Pabalan.²⁷ Figure 4 illustrates $\log K_c$ against density for NaCl at 623 K, both in water and in steam. It shows the

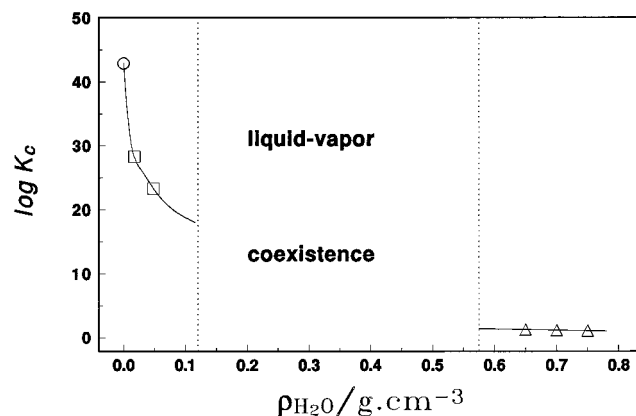


Figure 4. $\log K_c$ against density for NaCl in water at 623 K: (○) for pure NaCl vapor,²⁵ (△) from conductivity measurements,⁹ (□) present work.

two data points calculated by means of molecular dynamics simulation in the present work together with that of pure NaCl vapor²⁵ and those at higher fluid density obtained from conductivity measurements.⁹ The value for $\log K_c$ found in liquidlike densities must increase steeply with decreasing density in order to meet the value for the pure salt in the vapor phase when the density of H_2O tends to zero. Figure 4 suggests that this big and sudden change of slope would occur at densities corresponding to the region of coexistence of vapor and liquid phases. Thus at 623 K, the wide gap in densities that exists due to the vapor–liquid phase transition hampers a complete description of the density behavior. In spite of this the values of $\log K_c$ obtained by molecular dynamics for NaCl, which are plotted in Figure 4, may be considered to be in fair agreement with the available experimental information.

Solubility data for solid KCl and NaCl in subcritical steam are also scarce. Alekhin and Vakulenko²⁹ have reported data for KCl in steam; there is however some concern regarding their accuracy. Using the same experimental method, these authors have reported data for NaCl³⁰ which, when compared to those given by Pitzer and Pabalan for NaCl in steam,²⁷ appear to overestimate the solubility of solid NaCl, especially at subcritical temperatures; consequently it should be borne in mind that the data reported by Alekhin and Vakulenko can only be taken as indicative. Table 4 shows the value of the solubility of KCl and NaCl as mole fractions calculated with the molecular dynamics results together with experimental values. The data of Pitzer and Pabalan for NaCl at 623 K are 3–5 times smaller than the simulation results; notwithstanding this difference, it is considered that the simulation procedure describes satisfactorily the behavior of ions in steam. It is to be expected that our calculations give larger solubility than experiment because the SPC Hamiltonian was devised to describe condensed-phase water, where the H_2O molecules have a larger (effective) dipole moment than in vacuo. The last column of Table 4 reports the enhancement factors calculated from the solubility of salts determined with the molecular dynamics procedure.

The infinite dilution residual chemical potentials of ions and ion pairs in steam, defined by eq 3, describe the solvation of the gaseous ionic species transferred to steam at infinite dilution. Hence it is interesting to compare the thermodynamic quantities of hydration of ions in steam to those in water at different temperatures. Table 5 contains the experimental standard thermodynamic quantities of hydration of $\text{Na}^+ + \text{Cl}^-$ (i.e. as free ions) in water at several temperatures and those calculated from simulation for $\text{Na}^+ + \text{Cl}^-$ in steam at 623 K. It has been considered that for ionic species in liquid water the enthalpies

TABLE 5: Standard Gibbs Energy, Internal Energy, and Entropy of Hydration of Na⁺ + Cl⁻ (kJ mol⁻¹) in Water at Several Temperatures and in Steam at 623 K

state	$-\Delta_{\text{hyd}}G$	$-\Delta_{\text{hyd}}U$	$-T\Delta_{\text{hyd}}S$	ref
water, 298 K	720.1	773.4	53.2	<i>a</i>
water, 373 K	705.4	783.8	78.4	<i>a</i>
water, 473 K	682.0	801.6	119.6	<i>a</i>
water, 573 K	652.7	855.8	203.1	<i>a</i>
steam, state V	198.6	781.3	583	<i>b</i>
steam, state VI	270.1	968.2	698	<i>b</i>

^a Ref 31. ^b Present work. For calculation of $\Delta_{\text{hyd}}U$ and $T\Delta_{\text{hyd}}S$, see text.

of hydration are, to a good approximation, equivalent to the internal energies of hydration, which are the quantities obtained from simulation. The entropy of hydration for the two ions in steam, reported in the fourth column of Table 5, has been calculated with the assumption $\Delta_{\text{hyd}}H \approx \Delta_{\text{hyd}}U$. This is not a good approximation for systems in the vapor phase; hence the values reported in column four of Table 5 should be taken as maximum boundaries to $T\Delta_{\text{hyd}}S$ since the correction would make a negative contribution to it.

While the energy of hydration in steam has a magnitude similar to that found in liquid water, the chemical potential is much smaller in steam, as expected on the basis of the smaller solubility of salts in steam. As temperature increases, the chemical potential and entropy of hydration in liquid water gradually tend to those found in steam, but even at 573 K they are still qualitatively different. The most remarkable difference observed with the hydration of ions in dense water is the very large magnitude of the term $-T\Delta_{\text{hyd}}S$ for ions in steam. Hydration in steam is associated with a very large negative entropy term, which is a consequence of the electrostriction of water molecules, which leads to their accumulation in the neighborhood of the ions and limits their mobility. It is this very large reduction in entropy occurring in highly compressible steam that limits the solubility of ions in steam, not changes in the energy of hydration. While in dense fluids electrostriction mainly affects the orientational structure of solvent molecules surrounding the ions, in steam the considerable increase in the local density is the most characteristic feature of ion solvation.

A final comment with reference to the thermodynamics of hydration of ions in small H₂O clusters which surround the ions, studied by Kebarle and coworkers,²⁰ is worthwhile. This important information refers to rather well-defined *solvates* of the ions, as shown by the constancy of $\Delta_{\text{hyd}}H$ over a wide temperature range. The energetics of these small clusters bears a closer relation to the concept of a compact first solvation shell,

which is normally applied to ions in high-density polar liquids. On the other hand, ions in steam do not show such a clear hydration shell due to the lower packing fraction of the fluid. This contention is supported by the values calculated in this work for the residual thermodynamic quantities.

Acknowledgment. I am very grateful to Drs. D. Laria and H. Corti for reading the manuscript and making helpful suggestions. I also thank CONICET and UBACyT for partial economic support.

References and Notes

- (1) Neilson, G. W.; Enderby, J. E. *Proc. R. Soc.* **1983**, A390, 353.
- (2) Neilson, G. W.; Enderby, J. E. *J. Phys. Chem.* **1996**, 100, 1317.
- (3) Yu, J. A.; Karplus, M. *J. Chem. Phys.* **1988**, 89, 2366.
- (4) Quint, J. R.; Wood, R. H. *J. Phys. Chem.* **1985**, 89, 380.
- (5) Wood, R. H.; Quint, J. R. *J. Phys. Chem.* **1989**, 93, 936.
- (6) Fernández-Prini, R.; Japas, M. L. *Chem. Soc. Rev.* **1994**, 23, 155.
- (7) Re, M.; Laria, D. *J. Phys. Chem.*, in press.
- (8) Margulis, C.; Laria, D.; Fernández-Prini, R. *J. Chem. Soc., Faraday Trans.* **1996**, 92, 2703.
- (9) Ho, P. C.; Palmer, D. A.; Mesmer, R. E. *J. Solut. Chem.* **1994**, 23, 997.
- (10) Quist, A. S.; Marshall, W. L. *J. Phys. Chem.* **1968**, 72, 684.
- (11) Fernández-Prini, R.; Japas, M. L.; Corti, H. R. *Pure Appl. Chem.* **1993**, 65, 913.
- (12) Berendsen, H. J. C.; Postma, J. P. M.; von Gunsteren, W. F.; Hermans, J. *Intermolecular*; Reidel: Dordrecht, 1981.
- (13) Welch, D. O.; Lazareth, O. W.; Dienes, G. J. *J. Chem. Phys.* **1976**, 64, 835.
- (14) Pettitt, B. M.; Rossky, P. J. *J. Chem. Phys.* **1986**, 84, 5836.
- (15) Laria, D.; Fernández-Prini, R. *J. Chem. Phys.* **1995**, 102, 7664.
- (16) Andersen, H. C. *J. Chem. Phys.* **1980**, 72, 2384.
- (17) Ryckaert, J. P.; Ciccotti, G.; Berendsen, H. J. C. *J. Comput. Phys.* **1977**, 23, 327.
- (18) Fernández, D. P.; Goodwin, A. R. H.; Lemmon, E. W.; Levelt Sengers, J. M. H.; Williams, R. C. *J. Phys. Chem. Ref. Data* **1997**, 26, 1125.
- (19) Böttcher, C. J. F. *Theory of Electric Polarization*. Elsevier: New York, 1973; Vol. I.
- (20) Arshadi, M.; Yamdagni, R.; Kebarle, P. *J. Phys. Chem.* **1970**, 74, 1475.
- (21) Kirkwood, J. G. *J. Chem. Phys.* **1935**, 3, 300.
- (22) Rowlinson, J. S.; Swinton, F. L. *Liquids and Liquid Mixtures*; Butterworths: London, 1982.
- (23) Cui, S. T.; Harris, J. G. *J. Phys. Chem.* **1995**, 99, 2900.
- (24) Dejaegere, A.; Karplus, M. *J. Phys. Chem.* **1996**, 100, 11148.
- (25) Stull, D. R.; Prophet, H. *JANAF Thermochemical Tables*; NSRDS-NBS 37, 1971.
- (26) Franck, E. U. *Z. Phys. Chem. N.F.* **1956**, 8, 192.
- (27) Pitzer, K. S.; Pabalan, R. T. *Geochim. Cosmochim. Acta* **1986**, 50, 1445.
- (28) Laria, D.; Fernández-Prini, R. *Chem. Phys. Lett.* **1993**, 205, 260.
- (29) Alekhin, Y. V.; Razina, M. V.; Vakulenko, A. G. *Third International Symposium on Hydrothermal Reactions*; Summary 1–2; Frunze, Kirghizia, USSR, 1989.
- (30) Alekhin, Y. V.; Vakulenko, A. G. *Geokhim.* **1987**, 1468.
- (31) Sen, U. *J. Chem. Soc., Faraday Trans. 1* **1981**, 77, 2885.